lubricants

MDPI

Article

Microstructural and Chemical Characterization of the Tribolayer Formation in Highly Loaded Cylindrical Roller Thrust Bearings

Carsten Gachot [1,*], ChiaJui Hsu [1], Sebastián Suárez [1], Philipp Grützmacher [1], Andreas Rosenkranz [1,2], Andreas Stratmann [3] and Georg Jacobs [3]

[1] Department of Material Science and Engineering, Saarland University, Saarbrücken 66123, Germany; chiajui.hsu@uni-saarland.de (C.H.); s.suarez@mx.uni-saarland.de (S.S.); philipp.gruetzmacher@uni-saarland.de (P.G.); a.rosenkranz@mx.uni-saarland.de (A.R.)

[2] Department of Physics, Pontifical Catholic University of Chile, Santiago de Chile 7820436, Chile

[3] Institute for Machine Elements and Machine Design, RWTH Aachen, 52062 Aachen, Germany; stratmann@ime.rwth-aachen.de (A.S.); jacobs@ime.rwth-aachen.de (G.J.)

* Correspondence: c.gachot@mx.uni-saarland.de; Tel.: +49-0681-302-70554; Fax: +49-0681-302-70502

Academic Editors: Werner Oesterle and Ga Zhang
Received: 24 March 2016; Accepted: 18 May 2016; Published: 8 June 2016

Abstract: Zinc dithiophosphates (ZDDP) have been widely applied in automobile industry for over 70 years as a lubricant additive for wear protection. Tribolayers have been described as blue- and brown-colored layers on surfaces observed by microscopical observation or even bare eye presumably as a consequence of layer thickness or chemical composition. However, the reaction pathways of ZDDP tribolayers are still not yet fully understood. In the present study, the difference between the blue- and brown-colored tribolayers has been revealed by high resolution methods in cylindrical roller thrust bearings at relatively high contact pressures of around 1.92 GPa. After running a FE8 standard bearing test with a normal load of 80 kN and a temperature of 60 °C, said tribolayers could be identified on the bearing surfaces. By using Raman spectroscopy, it could be shown that the blue-colored layers are enriched by FeS and ZnS whereas the brown-colored layers show a significant amount of Fe_3O_4. This is an interesting finding as it clearly shows a correlation between the color appearance of the films and the chemical composition besides potential film thickness variations. Finally, transmission electron microscopy verified the amorphous nature of the formed tribolayer which is in a good agreement with literature.

Keywords: Lubrication; additives; ZDDP; tribolayer; bearings; microstructure

1. Introduction

Nowadays, there is pushing demand in fuel economy for passenger vehicles in order to fulfill legislative requirements for CO_2 emissions. This in turn leads to the introduction of ultra-low viscosity lubricants which could be one efficient way for lubricants to contribute to the fuel economy performance of passenger cars by reducing shear forces. However, a decrease in lubricant viscosity will result in thinner oil films and thus it will be more difficult for the oil to keep the loaded contacts efficiently apart from each other. This may imply a transition from full film to mixed lubrication with potentially accelerated wear rates and locally increased friction [1]. In order to avoid detrimental impacts on the engine and all its components it is necessary to add for example extreme pressure (EP) or anti wear (AW) additives which have the ability to form friction and wear reducing tribolayers [1]. However, the prediction of the forming tribolayers is highly complicated by operating conditions such as load, speed, and temperature. For that reason, additives are used in high concentrations to guarantee the formation and durability [2]. In this context, zinc dithiophosphates (ZDDPs) are widely

used as lubricant additives. The triumphal procession of ZDDP in the automotive industry already started more than 70 years ago [3]. ZDDP acts as an anti-wear agent, antioxidant, and corrosion inhibitor by decomposing peroxide and effectively destroying peroxy radicals. Interestingly, also the reaction products of ZDDP with peroxide and the respective radicals are again strongly efficient in corrosion inhibition [3]. The friction reducing properties of ZDDP are mainly attributed to an increased load support, beneficial mechanical properties by preferential shearing, removal of Fe_2O_3 particles, and finally the surface protection against corrosion. The growth and removal rate of the tribolayers is a highly dynamic process [4].

Apart from the abovementioned positive effects of ZDDP as a lubricant additive, it is well known that sulphur and phosphorous oxides as well as ash may negatively affect the effective life of exhaust catalysts [1]. Additionally, due to phosphorous and sulphur limits in engine oil specifications, it is considered to progressively reduce the usage of ZDDP or even to replace it [5]. A successful reduction or replacement certainly needs a thorough understanding of the governing mechanisms. It is well known that effective tribolayers can be realized by thermal or tribomechanical activation in loaded contacts [6]. Fujita and Spikes studied the morphology of the tribolayers for different temperatures and contact pressures up to 950 MPa [6]. They could show that pronounced tribolayers under thermal activation are only possible at temperatures higher than 150 °C, whereas loaded conditions already yield in an efficient tribolayer at room temperature. Although quite similar regarding their composition, Bancroft *et al.* proved that the tribomechanically induced reaction layers are more wear resistant than the thermally activated layers [7].

A closer look at the layer morphology shows some important aspects. According to the well-established model by Schmaltz, the boundary layer system typically consists of an inner and outer boundary layer [8]. The inner layer (tribomutation layer) is a fine-crystalline zone resulting from finishing processes or surface deformations with a thickness around 400 nm up to 5 µm (depending on operating conditions). In contrast to that, the outer boundary layer is composed of an oxide layer (<100 nm) followed by a reaction- or tribolayer (<150 nm thickness) and finally an adsorption layer on top [8]. The reaction layer is particularly interesting as it is responsible for the friction and wear reduction. Usually, this reaction layer is rough and patchy mainly composed of pyro- and orthophosphate glasses on the bulk level with an additional nanoscale layer of zinc polyphosphates and a sulphur-rich layer of typically 20 nm close to the metal surface [9]. Over the years, lots of microstructural studies and investigations related to the chemical nature of the reaction layers were done. In particular, Martin *et al.* applied analytical techniques such as electron energy loss spectroscopy (EELS), X-ray adsorption fine structure analysis (EXAFS) or X-ray absorption near-edge spectroscopy (XANES) to reveal the chemical composition and structure of said layers [10–13]. Despite the use of high resolution and sophisticated analytical methods, there is still a controversial issue concerning the specific reaction pathways and kinetics of the ZDDP layer formation [1]. Some recent progress was made by using, for example, classical molecular dynamics simulations (MD simulations) coupled with tight binding quantum chemical MD [14]. Mosey *et al.* explained the positive effects of ZDDP by a cross-linking of phosphates under sufficiently high contact pressure [15]. Gauvin *et al.* and Berkani *et al.* could experimentally verify the simulations by spectroscopic methods under contact pressures of up to 7 GPa [16,17]. However, studies referring to the transfer of these findings to highly loaded cylindrical roller thrust bearings are scarce in literature. Moreover, the role and origin of typically observed blue- and brown-colored films on the contacting surfaces are still not fully understood. According to Hsu, the different colors of the layers (e.g., blue or brown films) are due to thickness differences [18].

In this research contribution, we would like to study those brown- and blue-colored films in highly loaded cylindrical roller thrust bearings in more detail by various advanced and high resolution techniques such as Raman spectroscopy and transmission electron microscopy (TEM). For a given load of 80 kN and an operating temperature of 60 °C in a roller bearing lubricant test rig (FE8 test according to DIN 51819-3 [19]), the speed, as one decisive factor for the film formation, was varied between 10, 15, and 20 rpm. Below 10 rpm, at the given load and temperature, no protective tribolayer can be

detected [20]. With increasing speed, there is a shift in the amount of blue- and brown-colored regions. As the appearance of blue and brown regions on the loaded surfaces usually indicates the successful formation of the wear protective tribolayer and is also most pronounced for the highest applied speed at 20 rpm, a stronger emphasis is put on analyzing said colored regions for this particular speed within this research work.

2. Experimental Section

2.1. Materials and FE8 Testing

In the present study, tribofilms were formed at the interface of cylindrical thrust roller bearings (Type 81212), made of a 100Cr6 bearing steel (52100) with the nominal chemical composition provided by the supplier (see Table 1, by applying a modified FE8 test corresponding to DIN 51819-3 [19]. A mineral oil of class ISO VG 100 is used as base oil and mixed with ZDDP additive. During the test, abundant lubricant was delivered to the area of contact by a circulation pump. In this study, rotational speed was adjusted at 10, 15, and 20 rpm with 10 rpm as a lower limit below which no tribolayer was induced at the given testing conditions. The test was run at 60 °C with an axial load of 80 kN, which corresponds to a Hertzian pressure of 1.92 GPa. The total testing time was 2 h. After the test, the surface was cleaned by using benzene and isopropanol to remove the residual lubricant, abrasives, and contaminants.

Table 1. Chemical composition (in wt %) of 100Cr6 (52100) bearing steel provided by the supplier.

Cr	C	Mn	Si	P_{max}	S_{max}	Cu_{max}	Mo_{max}	Al_{max}
1.35–1.6	0.9–1.05	0.25–0.45	0.15–0.35	0.025	0.015	0.3	0.1	0.05

2.2. Chemical Analysis

Chemical properties have been examined by Raman spectroscopy equipped with a grating of 2400 lines· mm^{-1} and a spectral resolution up to 1.2 cm^{-1}. 532 nm excitation wavelength laser source was provided with a power of 50 mW, and set as 10% of energy to prevent thermal effect to the tribolayer. The spectrum between 200 and 1500 cm^{-1} Raman shift has been obtained within 20 s acquisition time. After Raman acquisition, the spot focus had been examined by optical microscopy in order to check that there is no damage due to the laser beam exposure. The laser beam was focused on the surface by a 50× object lens with a final spot size of nearly 4 μm^2 for the subsequent analysis of the different colored regions of the worn ring surface. Moreover, energy dispersive X-ray spectroscopy (EDS) was used to examine the chemical composition in blue- and brown-colored regions. For that purpose, EDS line scans were performed at 20 kV and 100 kV (TEM-EDS) electron voltage and a dwell time of 2400 ms. By marking the respective positions, the resulting EDS line scans were compared with light microscopic images.

2.3. Topography and Microstructural Analysis

The overall morphology and topography were obtained by using light microscopy (Olympus BX 60, location) and white light interferometry (WLI, Zygo NewView 7300, location).

Scanning electron and focused ion beam microscopy (SEM/FIB, Dual Beam workstation Helios NanoLab FEI, location) were applied to observe the morphological properties on the surface and to prepare thin foils for subsequent analysis by TEM. A JEOL 2010F TEM was used for investigating the tribofilm morphology in more detail and diffraction images were collected to prove the amorphous/crystalline nature of the tribofilm.

3. Results and Discussion

Systematic studies on the tribofilm formation using ZDDP as an additive are rather scarce for highly loaded contacts *i.e.*, contact pressure higher than 1 GPa. For that reason, the tribolayer formation

on the surface of highly loaded cylinder roller thrust bearing rings at 1.92 GPa has been examined in the present study by high resolution and complementary characterization techniques. The tribological behavior of the used mineral oil of class ISO VG 100 mixed with ZDDP was tested in a modified FE8 test rig (DIN 51819-3). Here, the test rig is modified in terms of torque measurement and axial load supply which is done hydraulically [20]. Two cylindrical roller thrust bearings of type 81212 are used for the classification test due to the high percentage of slippage between washer and roller. The bearing and the quantitative run of the sliding speed curve as well as the FE8 test rig setup are shown in Figure 1. The axial load can be applied dynamically and under different operating conditions during one test. More details about the test rig and the experimental procedure can be found in [20].

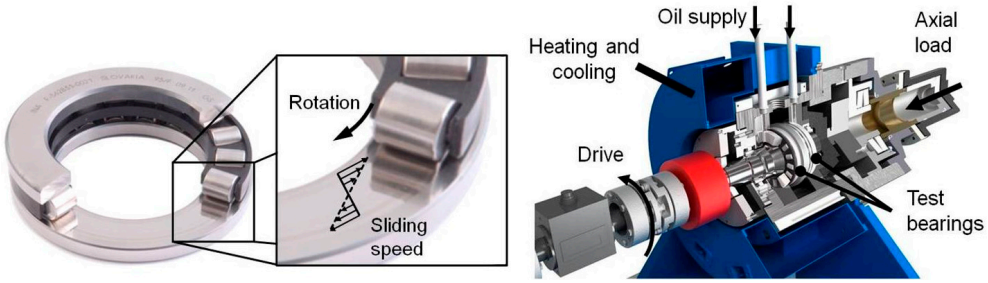

Figure 1. Cylindrical roller thrust bearing 81212 and modified FE8 test rig.

Figure 2 shows an overview of typical wear tracks recorded by optical light microscopy after having run the modified FE8 test for bearings for two hours and different rotational speeds (10, 15, and 20 rpm). Here, 10 rpm represents a lower limit for the tribolayer formation. At the given experimental conditions *i.e.*, load, temperature and additive concentration, no tribolayer will be built up below 10 rpm [20]. In the figure, the radial direction is from left to right (from inner to outer diameter). The differently colored regions (grey-for the substrate-brown-blue-yellow-blue-brown and grey again) can be clearly indentified along the radial direction for all tested rotational speeds.

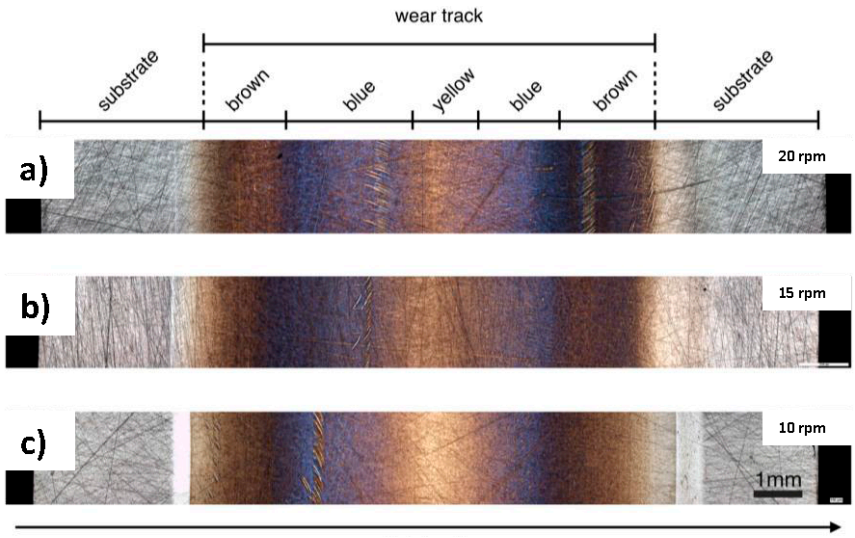

Figure 2. Overview of the wear track on the surface of the thrust ring, after FE8 test by applying a rotational speed of 20 rpm (**a**); 15 rpm (**b**) and finally 10 rpm (**c**) with an axial pressure load of 80 kN and working temperature of 60 °C.

Except the grey regions, which are considered substrate without wear, the other three colored regions which had intensive contact to the cylindrical rollers during the test are completely located in the wear track. The emerging bright bands at lower speeds are wear tracks with abrasive and adhesive

wear. Due to the highest sliding speeds at the sides of the wear track, this area is highly critical with respect to wear. The inner track is even more critical as the smallest rolling speed and consequently the highest ratio of solid body contact can be found in this part. Because of that, the wear track at the inner part is more pronounced (Figure 2c). The width of the roller (11 mm) exceeds the one of the wear track (~9 mm). The contact width between roller and washer is about 10–10.5 mm and includes the area of wear in Figure 2c.

The transition zones between different regions are quite diffuse and partially overlapping to some extent. With increasing rotational speed, the amounts of blue- and brown- colored regions are changed narrowing the yellow central part of the ring. For 20 rpm, the blue zone is more intense compared to lower rotational speeds. For that reason, the analysis of the layers in the following will be focused on that particular speed. By using a higher magnification (see Figure 3), the blue-film region appears more patchy like "islands" and not as a homogeneous layer. Additional topographical parameters such as root mean square roughness (rms) and peak to valley (PV) distance of the blue and brown films were obtained by white light interferometry from the inner and outer segments (see Table 2). The pristine arithmetic surface roughness of the steel substrate is R_a, steel ~0.2 µm. The roughness decreases with the formation of the tribolayers, partially covering the visible grinding marks of the substrate (see Figure 2). However, there is neither a tendency for the rms value nor the PV distance for the differently colored regions as a function of rotational speed as can be seen in Table 2. However, roughness generally plays an important role for the tribolayer formation in boundary lubricated contacts. Tribolayers usually form faster and require less energy input to be formed for a rough surface compared to a smooth surface [4].

Table 2. Parameters of FE8 test and root mean square roughness (rms) and peak to valley (PV) distance for the tribolayers. The arithmetic roughness R_a of the steel substrate is around 0.2 µm.

Rotational Speed (rpm)	Load (kN)	Working Temp. (°C)	Blue-Film				Brown-Film			
			Inner		Outer		Inner		Outer	
			Rms (nm)	PV (µm)	Rms (nm)	PV (µm)	Rms (nm)	PV (µm)	Rms (nm)	PV (µm)
10	80	60	31 ± 2.5	1.6 ± 1.0	30 ± 1.4	0.8 ± 0.2	66 ± 2.5	2.6 ± 0.2	47 ± 1.2	3.3 ± 0.7
15	80	60	40 ± 3.6	0.7 ± 0.1	47 ± 7.8	1.1 ± 0.6	42 ± 4.7	0.6 ± 0.1	42 ± 0.6	1.1 ± 0.9
20	80	60	41 ± 2.0	1.5 ± 0.8	42 ± 6.8	2.0 ± 0.8	58 ± 2.1	2.0 ± 0.2	53 ± 4.4	2.1 ± 0.2

Lubricant mineral oil mixed with ZDDP additive, C3C4-alkyl-chain with 0.05% P, 2 h sliding test.

Figure 3 displays the results of an EDS line-scan, which shows the distribution of typically occurring elements such as Zn, S, or P. In the figure, dots and triangles are used to represent the position of blue- and brown-colored regions. Along the scan-line, blue and brown film regions are mixed up thus complicating the analysis. Here, the content of Zn, P, and S rise while scanning through the blue-film region. On the other hand, in the brown-film region, only sulphur shows a slightly higher content.

Deeper information regarding the chemical bonding within the tribolayer was acquired with the help of Raman spectroscopy. In Figure 4, Raman spectra taken between 200 and 1500 cm^{-1} show the resonance peaks present at the yellow-, blue- and brown-colored regions, as well as the substrate. As a reference, the spectrum of the substrate showed the typical peaks to Cr-O and Fe-O, without revealing neither phosphates nor sulphides. In the yellow region, the spectrum mainly shows iron oxide (Fe_3O_4) at around 680 cm^{-1} and some sulphides. The Cr-O peaks (native oxide of the steel) of the substrate were not observed, presumably either due to the covering of this phase with other or a higher Raman activity of Fe_3O_4. Compared to the substrate, the blue and brown film regions display pronounced P-O, Fe-S, and Zn-S resonance peaks. The broad band at 1000 cm^{-1} is related to polyphosphates including three sub-peaks at 965, 1007, and 1045 cm^{-1} [17]. Additionally, the band at 386 cm^{-1} corresponds to FeS [21], whereas the peak at 351 cm^{-1} corresponds to ZnS [22]. Since Raman spectroscopy is a volume-sensitive technique, the analysis must be performed by comparing intensity

ratios. In this sense, a comparison of the blue and brown films is carried out by relating the intensities of the $(Zn_{0.88}Fe_{0.12})S_{1.00}$ band (351 cm^{-1}) [23] and the FeS band at 386 cm^{-1} (Figure 5). By comparing the intensity ratio of the aforementioned bands for both regions, it can be stated that this intensity ratio is higher for the blue film, indicating a higher $(Zn_{0.88}Fe_{0.12})S_{1.00}$ relative content. Furthermore, higher relative peak intensity for Fe_3O_4 is noticed for the brown-colored region, whereas no evident difference in the polyphosphate signal can be detected in the Raman spectra for both regions. This is a significant finding between the different colored regions, emphasizing that the color difference could be strongly attributed to the chemical composition instead of the layer thickness, as previously assumed in the literature [18].

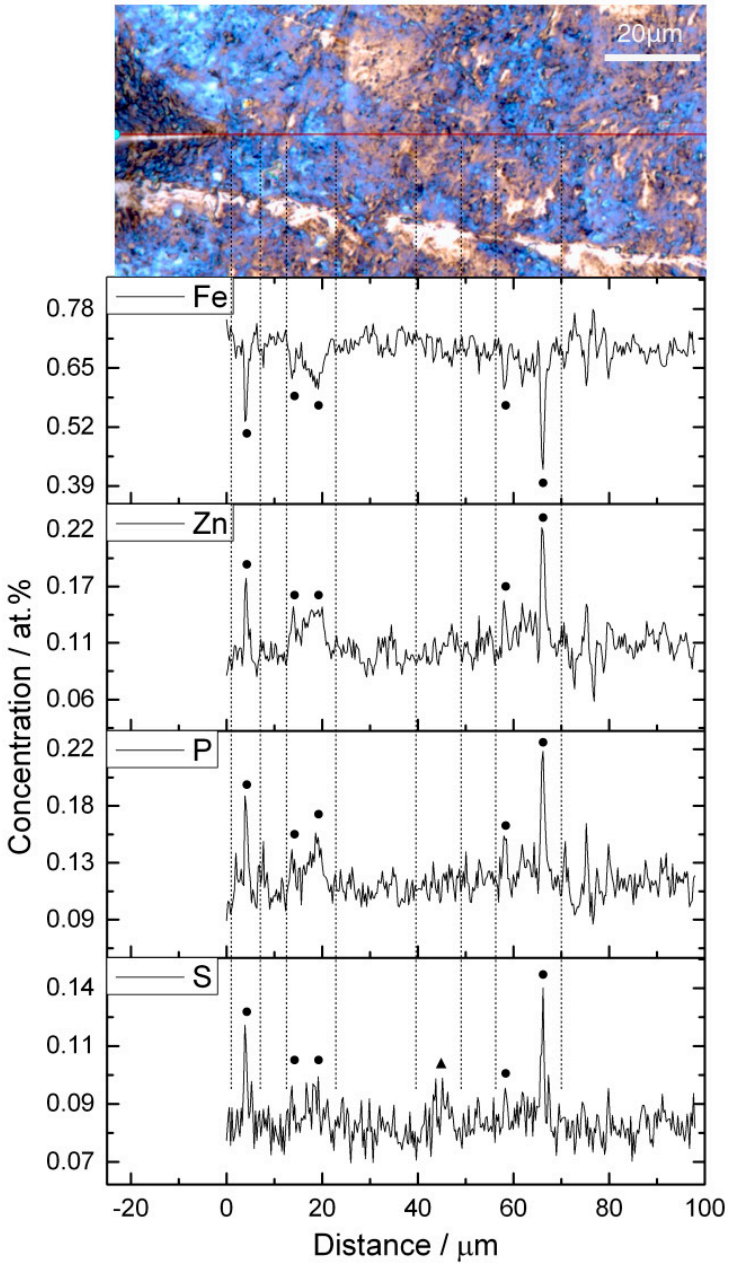

Figure 3. EDS line-scan through blue (dots) and brown film (triangle) regions at a rotational speed of 20 rpm.

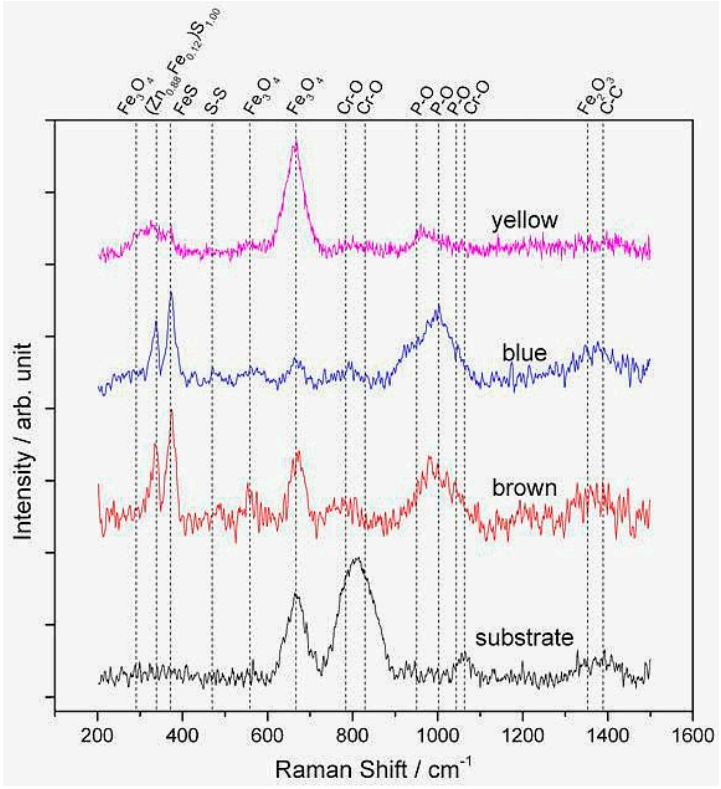

Figure 4. Raman spectra of anti-wear film at a fixed rotational speed of 20 rpm in the Raman shift range from 200 to 1500 cm^{-1}.

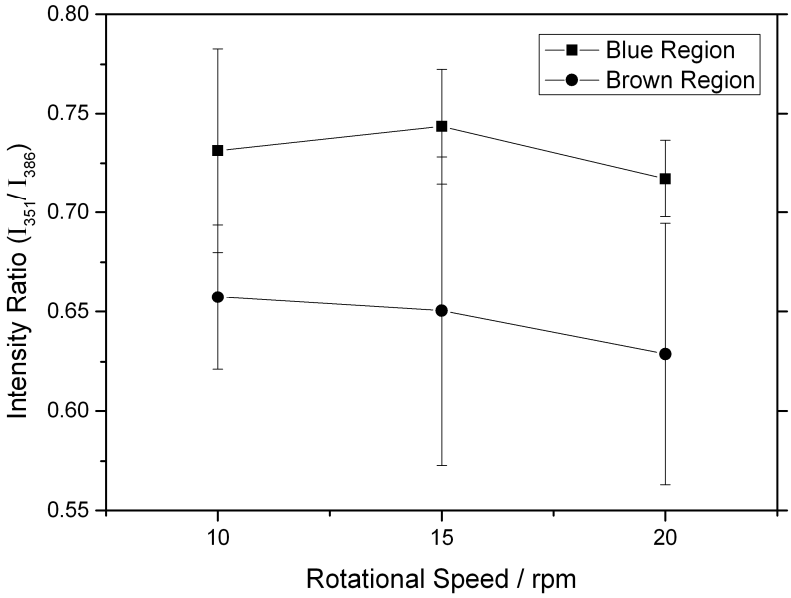

Figure 5. Intensity ratio of the peak attributed to $(Zn_{0.88}Fe_{0.12})S_{1.00}$ (351 cm^{-1}) over the peak of FeS (386 cm^{-1}), between Raman spectra of blue and brown film regions.

Figure 6a shows a bright-field electron micrograph of the analyzed zone. Four different regions are noticed being from top-right to bottom-left: Ion-deposited Pt protective layer, electron beam-deposited Pt protective layer, the respective tribolayer, the tribomutation layer and finally the steel substrate. The protective Pt layers are necessary for the FIB preparation in order to avoid damaging the region of interest. The bright tribolayer has a thickness between 70 and 140 nm and the deformed tribomutation

layer between 250 and 450 nm which is in a good agreement with values listed in literature [8]. The thickness mainly varies because of roughness differences and the subjected loading profile (see Figure 1 magnified insert) from the inner to outer ring segment. Selected area electron diffraction (SAED) was performed on two regions of interest (the tribolayer and the substrate) at 200 kV with a diffraction aperture of 180 nm. The diffraction pattern of the tribolayer (Figure 6b) resembles an amorphous structure, with some reflections from the substrate. This is an unavoidable feature, due to the aforementioned size of the diffraction aperture of 180 nm. The diffraction pattern of the substrate (Figure 6c) has been indexed and fully corresponds to ferrite (ICDD International Centre for Diffraction Data, PDF-2-file: 06-0696), being observed the main six reflections. The layered structure and the amorphous nature of the tribolayer fits well to the layer model proposed by Schmaltz and Bec *et al.* who describe the existence of a fine-crystalline and deformed tribomutation layer followed by a crystalline layer of sulphides and oxides and finally an amorphous tribolayer consisting of polyphosphates on top [8,24]. The crystalline layer of sulphides and oxides cannot be clearly identified in the TEM image. The typical thickness of this layer would be about 20 nm [24]. In contrast to that, the tribomutation layer is well pronounced due to the relatively high Hertzian contact pressure of around 1.92 GPa. Furthermore, chemical analysis was performed on the substrate and the blue film region by TEM-EDS due to its higher spatial resolution compared to conventional SEM-EDS (see Figure 7). In Figure 7a, the presence of distinct Zn, P, and S peaks is visible compared to the substrate spectrum.

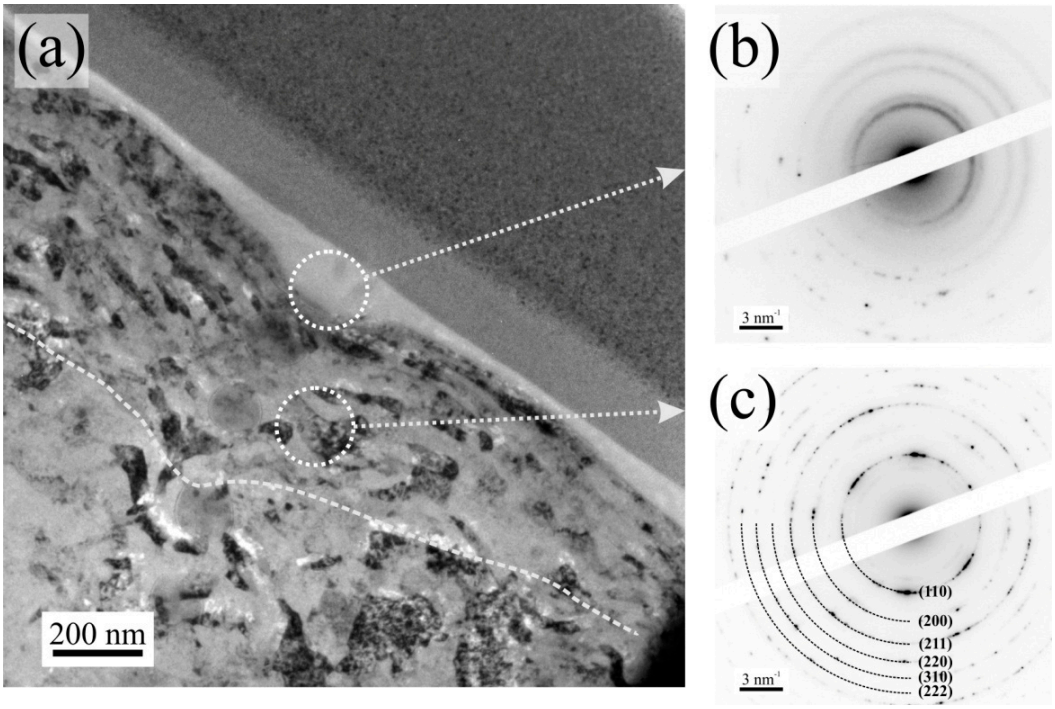

Figure 6. (**a**) Bright field TEM micrograph of the cross section of the wear track; (**b**) Electron diffraction pattern of the tribolayer; (**c**) Electron diffraction pattern of the substrate.

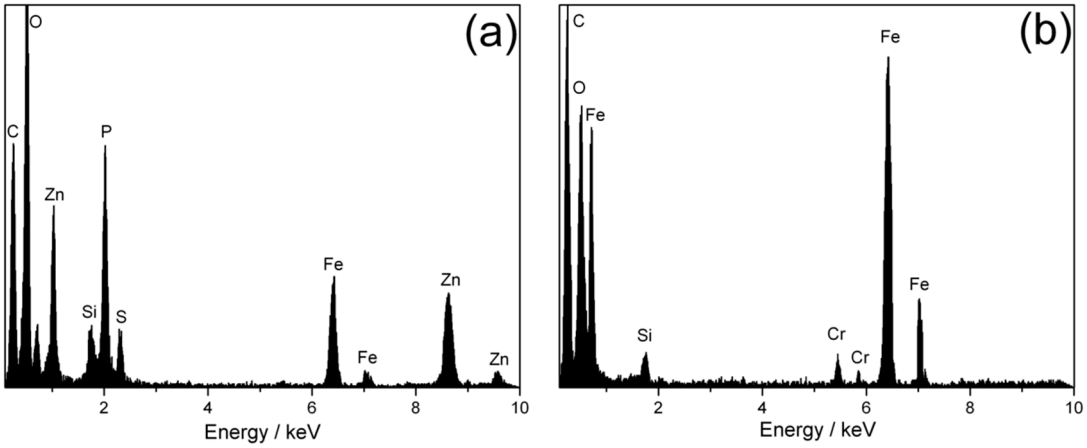

Figure 7. TEM-EDS spectra of blue-film region (**a**) and substrate (**b**).

The question regarding which film is more beneficial concerning the tribological performance cannot be answered in a straightforward manner. As soon as the colored tribolayers form (blue or brown), the bearings last until the end of the FE8 test without failing. The reaction pathways are still a matter of debate and the operating conditions provide a quite complex set of parameters with a difficult interplay between each other. By increasing the speed, more energy will be stored in the tribosystem and additionally the contact will be more effectively replenished with lubricant and so additive molecules thus facilitate the formation of potential wear resistant tribolayers. Mosey's MD simulations suggested a contact pressure induced cross-linking of zinc phosphate molecules [15]. According to Gosvami *et al.*, the nucleation and growth of tribolayers can be well described by a stress and thermally activated Arrhenius model. In this context, it is then assumed that the nucleation and growth are significantly influenced by surface heterogeneities, such as roughness, thus lowering the necessary activation energy for the tribolayer formation by varying contact areas and stresses [25]. On the other hand, a certain regeneration time between two rolling events is needed to allow for the formation of the layers [20]. With increasing speed, the time between two rolling events is shortened and therefore impeding the layer formation. It will be interesting to systematically elucidate the lower boundaries for the respective operating conditions under which a successful tribolayer can still be generated and to further reveal the reaction pathways of the tribolayers especially for highly loaded thrust bearings.

4. Conclusions

The tribolayer formation on the surface of highly loaded cylindrical roller thrust bearing rings at 1.92 GPa has been examined in a modified FE8 test for different rotational speeds. The resulting tribolayers were subsequently characterized by Raman spectroscopy, TEM, and TEM-EDS. The key findings of the research article may be summarized as follows.

- Below a rotational speed of 10 rpm no tribolayer was observed. Therefore, 10 rpm represents a lower boundary at the given operating conditions of 80 kN normal load and 60 °C temperature. With increasing speed, the amounts of blue- and brown-colored regions vary. The most intense blue color appearance could be found for 20 rpm. The blue layer is not homogeneous but patchy as reported in literature.
- Raman spectroscopy could prove that the blue-layers are enriched with ZnS and FeS whereas the brown layers are characterized by a larger amount of Fe_3O_4. As far as polyphosphates are concerned, no distinct differences could be found for both colored layers in the respective Raman spectra. This experimental finding reveals that the color appearance may be due to chemical composition and not only because of thickness effects. The question regarding the performance

differences of the blue- and brown-colored regions cannot be answered within this research work and will be part of a follow-up paper.

- Microstructural studies by TEM verified the layered morphology with a 250–450 nm thick deformed tribomutation layer followed by 70–140 nm thick amorphous tribolayer with clear signatures of Zn, P, and S based upon TEM-EDS measurements.

Acknowledgments: The present work is supported by funding from the Deutsche Forschungsgemeinschaft (DFG) in the priority program SPP 1551 "Resource efficient design elements" (DFG, project: GA 1706/2-2). The EU funding for the project AME-Lab (European Regional Development Fund C/4-EFRE-13/2009/Br) is gratefully acknowledged. Volker Presser (Raman spectroscopy, Saarland University) and Rainer Birringer (TEM, Saarland University) are both kindly acknowledged.

Author Contributions: Carsten Gachot wrote the article and analyzed the overall data. Chia Jui Hsu designed the experiments for optical microscopy and analyzed Raman data. Sebastián Suárez performed TEM experiments and analyzed data. Philipp Grützmacher performed Raman experiments and provided discussion on gained results. Andreas Rosenkranz analyzed EDS data and wrote experimental part. Andreas Stratmann designed the test rig, provided specimens and analyzed data for color formation depending on experimental conditions. Georg Jacobs supervised work, discussed the basic design of experiments with Andreas Stratmann and Carsten Gachot, provided suggestions for final discussion of data.

Conflicts of Interest: The authors declare no conflict of interest.

References

1. Spikes, H. The history and mechanisms of ZDDP. *Tribol. Lett.* **2004**, *17*, 469–489. [CrossRef]
2. Varlot, K.M.; Kasrai, M.; Martin, J.M.; Vacher, B.; Bancroft, G.M.; Yamaguchi, E.S.; Ryason, P.R. Antiwear film formation of neutral and basic ZDDP: Influence of the reaction temperature and of the concentration. *Tribol. Lett.* **2000**, *8*, 9–16. [CrossRef]
3. Spikes, H. Friction modifier additives. *Tribol. Lett.* **2015**, *60*, 1–26. [CrossRef]
4. Kubiak, K.J.; Mathia, T.G.; Bigerelle, M. Influence of roughness on ZDDP tribofilm formation in boundary lubricated fretting. *Tribol. Mater. Surf. Interfaces* **2012**, *6*, 182–188. [CrossRef]
5. International Lubricant Standardization and Approval Committee. *ILSAC GF-5 Standard for Passenger Car Engine Oils*; US/Europe/Japan, 2009.
6. Fujita, H.; Spikes, H.A. The formation of zinc dithiophosphate antiwear films. *J. Eng. Tribol.* **2004**, *218*, 265–278. [CrossRef]
7. Bancroft, G.M.; Kasrai, M.; Fuller, M.; Yin, Z.; Fyfe, K.; Tan, K.H. Mechanisms of tribochemical film formation: Stability of tribo and thermally generated ZDDP films. *Tribol. Lett.* **1997**, *3*, 47–51. [CrossRef]
8. Schmaltz, G. *Technische Oberflächenkunde*; Verlag von Julius Springer: Berlin, Germany, 1936.
9. Martin, J.M. Antiwear mechanisms of zinc dithiophosphate: A chemical hardness approach. *Tribol. Lett.* **1999**, *6*, 1–8. [CrossRef]
10. Martin, J.M.; Mansot, J.L.; Berbezier, I.; Dexpert, H. The nature and origin of wear particles from boundary lubrication with a zinc dialkyl dithiophosphate. *Wear* **1984**, *93*, 117–126. [CrossRef]
11. Martin, J.M.; Belin, M.; Mansot, J.L.; Dexpert, H.; Lagarde, P. Friction induced amorphization with ZDDP—an EXAFS study. *ASLE Trans.* **1986**, *29*, 523–531. [CrossRef]
12. Martin, J.M.; Mansot, J.L.; Berbezier, I.; Belin, M.; Balossier, G. Microstructural aspects of lubricated mild wear with zinc dialkyldithiophosphate. *Wear* **1986**, *107*, 355–366. [CrossRef]
13. Belin, M.J.; Martin, J. L.; Martin, J.M.; Mansot, J.L. Role of iron in the amorphization process in friction-induced phosphate glasses. *Tribol. Trans.* **1989**, *32*, 410–413. [CrossRef]
14. Onodera, T.; Martin, J.M.; Minfray, C.; Dassenoy, F.; Miyamoto, A. Antiwear chemistry of ZDDP: Coupling classical MD and tight-binding quantum chemical MD methods (TB-QCMD). *Tribol. Lett.* **2013**, *50*, 31–39. [CrossRef]
15. Mosey, N.J.; Woo, T.K.; Kasrai, M.; Norton, P.R.; Bancroft, G.M.; Müser, M.H. Interpretation of experiments on ZDDP anti-wear films through pressure-induced cross-linking. *Tribol. Lett.* **2006**, *24*, 105–114. [CrossRef]
16. Gauvin, M.; Minfray, C.; Belin, M.; Aquilanti, G.; Martin, J.M.; Dassenoy, F. Pressure-induced amorphization of zinc orthophosphate—Insight in the zinc coordination by XAS. *Tribol. Int.* **2013**, *67*, 222–228. [CrossRef]
17. Berkani, S.; Dassenoy, F.; Minfray, C.; Martin, J.M.; Cardon, H.; Montagnac, G.; Reynard, B. Structural changes in tribo-stressed zinc polyphosphates. *Tribol. Lett.* **2013**, *51*, 489–498. [CrossRef]

18. Hsu, S.M. Boundary lubrication of materials. *MRS Bull.* **1991**, *16*, 54–58.
19. DIN 51819-3. *Testing of Lubricants-Mechanical Dynamic Testing in the Roller Bearing Test Apparatus FE8—Part 3: Test Method for Lubricating Oils, Axial Cylindrical Roller Bearing*; 2005.
20. Stratmann, A. Formation of anti-wear films in rolling bearings due to run-in procedures. In Proceedings of the WTC 2013, Torino, Italy, 8 September 2013.
21. Ushioda, S. Raman scattering from phonons in iron pyrite (FeS_2). *Solid State Commun.* **1972**, *10*, 307–310. [CrossRef]
22. Brafman, O.; Mitra, S.S. Raman effect in wurtzite-and zinc-blende-type ZnS single crystals. *Phys. Rev.* **1968**, *171*, 931. [CrossRef]
23. Integrated Database for Raman Spectra, XRD and Chemistry Data of Minerals. Available online: http://www.rruff.info (accessed on 15 March 2016).
24. Bec, S.A.; Tonck, A.; Georges, J.M.; Coy, R.C.; Bell, J.C.; Roper, G.W. Relationship between mechanical properties and structures of zinc dithiophosphate anti-wear films. *Proc. R Soc. Lond. A Math. Phys. Eng. Sci.* **1999**, *455*, 4181–4203. [CrossRef]
25. Gosvami, N.N.; Bares, J.A.; Mangolini, F.; Konicek, A.R.; Yablon, D.G.; Carpick, R.W. Mechanisms of antiwear tribofilm growth revealed *in situ* by single-asperity sliding contacts. *Science* **2015**, *348*, 102–106. [CrossRef] [PubMed]

© 2016 by the authors; licensee MDPI, Basel, Switzerland. This article is an open access article distributed under the terms and conditions of the Creative Commons Attribution (CC-BY) license (http://creativecommons.org/licenses/by/4.0/).